Generation of Unagglomerated, Dense, $BaTiO_3$ Particles by Flame-Spray Pyrolysis

James H. Brewster and Toivo T. Kodas
Center for Micro-Engineered Materials, University of New Mexico, Albuquerque, NM 87131

Fine particles of dense, high-purity, crystalline $BaTiO_3$ were produced by flame-spray pyrolysis. A 0.5-M (Ba:Ti = 1:1) solution of barium acetate, titanium lactate, and water was aerosolized using an ultrasonic generator, and the droplets were delivered into the core of an annular diffusion flame (H_2/air) reactor. For all investigated temperatures [~1,000 – ~2,000°C adiabatic], the generated powders were chemically pure, crystalline (primarily tetragonal phase with hexagonal and cubic polymorphs), and unagglomerated. At a low-flame temperature (~1,000°C ad.), the particles produced were hollow and irregularly shaped. Particles produced at higher flame temperatures (> ~1,500°C ad.) were dense and homogeneous. Particles showed a transition from a nonspherical porous morphology to a spherical dense morphology with increasing temperature. By increasing residence time, the temperature at which particles became spherical and dense was reduced. Flame-spray pyrolysis provides a useful method for forming dense particles of high melting point materials by aerosol-phase densification.

Introduction

Barium titanate and other ferroelectric ceramics have applications in various fields because of their characteristics resulting from their spontaneous polarization. This has motivated many studies of the enhancement of the properties of barium titanate ceramics by controlling their microstructure (Arlt et al., 1985; Kinoshita and Yamaji, 1976; Lee and Kim, 1990). Because initial powder properties partially determine the microstructure of the final sintered ceramic, it is important to control the properties of the particles used as raw materials.

Many techniques exist for the production of metal oxide powders, most of which have been applied to barium titanate production (Colomban, 1985; Fang et al., 1990; Buchanan and Boy, 1987). Desirable powder characteristics, as a precursor to a sintered ceramic material, include small particle size (≤ 1 μm), no agglomeration, high purity, intraparticle homogeneity, high density, and sphericity. Of the various methods available for the production of metal oxide powders, spray pyrolysis provides most of these desirable characteristics without milling, which can introduce impurities, as discussed in the review by Kodas (1989). Spray pyrolysis is a powder-generation technique that involves the formation of precursor aerosol droplets that are delivered by a carrier gas through a heating zone. Inside the heating zone, the solvent evaporates and reactions occur within each particle to form a product particle. The resulting particles are then captured by a filter or other collection apparatus.

One major disadvantage of the spray pyrolysis method is the frequent production of hollow and/or porous particles (Gurav et al., 1993; Kodas, 1989; Ortega et al., 1991; Rossetti, Jr., et al., 1989). These particle morphologies are undesirable during sintering due to low green densities and extensive grain growth (Edelson and Glaeser, 1988). Many steps have been taken to combat this problem with differing degrees of success, including controlling droplet evaporation rate, adding colloidal seed particles, high-temperature aerosol-phase densification, and various chemical changes to the precursor solution (Gurav et al., 1993; Ortega et al., 1991). In this study, flame-spray pyrolysis, similar to the study by Zachariah and Huzarewicz in 1991, was investigated as a potential solution to problems facing conventional spray pyrolysis. In flame-spray pyrolysis, the heating zone consists of a chemical flame. This offers several advantages over a hot-walled furnace, including higher operating temperature, faster heating and cooling rates, more economical operation, and easier scale-up. The first advantage, higher operating tem-

Correspondence concerning this article should be addressed to T. T. Kodas.

perature, can potentially solve the previously noted problem encountered in conventional spray pyrolysis, which is the frequent formation of hollow particles. By operating at a temperature higher than the material's melting point, solid particles can be produced. Also, intraparticle homogeneity is improved by complete melting of the material. Crystallite size can also be controlled by melting the particles and regulating their cooling rate.

In this work we have shown that solid particles of a material with a high melting point (M.P. $BaTiO_3 = 1620°C$) could be produced by flame-spray pyrolysis. There have been many previous studies concerning particle generation using flame burners that refer to the formation of nanosized particles of metal oxides by gas-to-particle conversion of a volatile precursor. However, very few studies have been conducted on particle formation by intraparticle reaction within a flame. In other words, passing aerosolized precursor droplets through a flame reactor to form micrometer-sized ceramic particles has not been studied, save for the investigation of $YBa_2Cu_3O_{7-x}$ (1-2-3) superconducting ceramic particle formation by Zachariah and Huzarewicz in 1991. The purpose of this work was to gain a qualitative understanding of ceramic particle formation using the flame-spray technique. This includes understanding how various material properties and flame conditions affected particle morphology and crystallinity in a qualitative sense. The main motivation lies in that there are many advantages of flame-spray pyrolysis over conventional spray pyrolysis. The flexibility of this technique was also demonstrated in terms of altering the morphology, crystallinity, size, and surface area of the final powder.

Experimental Studies

The experimental apparatus consisted of an aerosol-generation section, a reactor section, and a powder-collection section. A 0.5-M (Ba:Ti = 1:1) solution of barium acetate, titanium lactate [dihydroxybis (ammonium lactato) titanium] (Tyzor LA), and water was used as the precursor. Aerosol generation was accomplished by using an ultrasonic generator (modified Holmes home humidifier as described in Gurav et al., 1993). The aerosol carrier gas, air, provided additional oxygen for the flame. The reactor section consisted of a concentric tube diffusion flame burner (Figure 1) attached to a vertically mounted 46-cm GE quartz tube (9 cm OD, 8.5 cm ID). The aerosol flow (0.5 to 2.0 SLPM) entered through the center tube (1/2 in. OD), the hydrogen flow (7.0 SLPM to 3.3 SLPM) entered through the first annulus, and pure air (21.5 SLPM) entered through the outer annulus. The flame was always operated in an O_2-rich condition (29% to 171% excess O_2) for safety considerations.

Flame temperature was controlled by altering the fuel/air mixture while keeping the total volumetric gas flow rate constant. Figure 2 is a plot representing the calculated adiabatic flame temperature vs. % excess O_2. These calculations were used to estimate the particle-formation temperature. Also shown are measured reference temperatures at two different locations (Figure 1) in the reactor vs. a normalized H_2 flow, where $Q(H_2)_{max} = 7.0$ SLPM. The indicated measured temperatures were much lower than the adiabatic flame temperature, because the thermocouples were not located within the flame region. In fact, because a diffusion flame was used, actual local flame temperature may have been hotter than

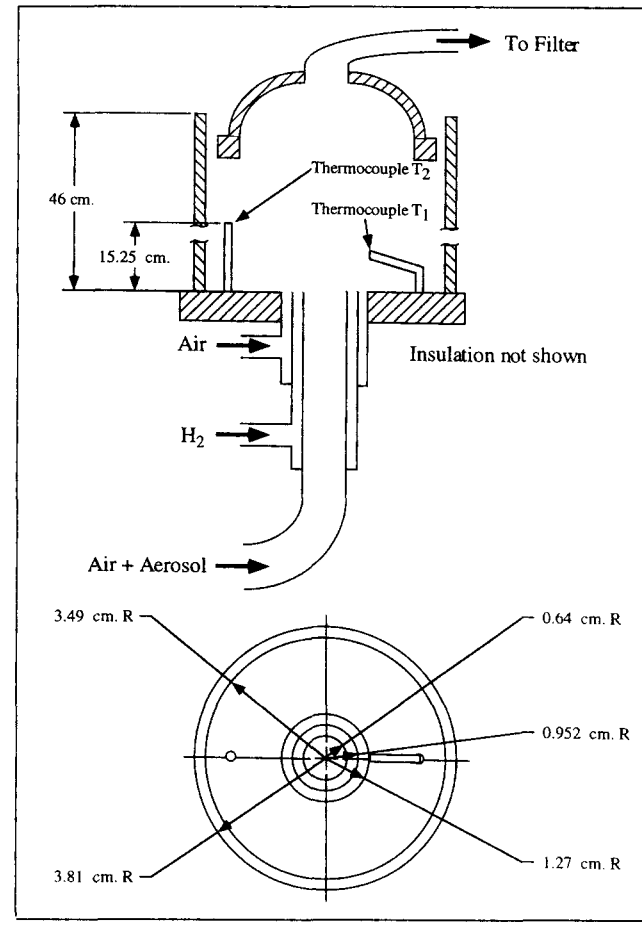

Figure 1. Flame reactor.

the calculated adiabatic flame temperature. Therefore, this can only represent an estimate as to what temperature the particles actually experienced.

The residence time was controlled by varying the aerosol flow rate. Because the evaporation and reaction of the aerosol droplet occurred within the non-fully developed entrance region of the flame reactor, a crude estimate for the residence time was assumed using the following general formula:

$$t_{res} = \frac{\pi d^2 L}{4Q}\left(\frac{T_i}{T_f}\right). \quad (1)$$

Alumina-insulated Pt/Pt 10% Rh fine wire thermocouples (type S) without radiation shielding were used to measure the flame reactor temperatures. The powder collection section consisted of an open bell collector leading to a stainless-steel filter holder. A vacuum pump provided flow through the collection system. The Tuffryn membrane filter (142 mm dia., 0.45 mm pore dia.) was supported on a Gelman 147-mm-diameter filter holder that was maintained at a temperature of 60–65°C.

Various characteristics of the powder were examined. Particle morphology was determined by transmission electron microscopy (TEM; JEOL 2000FX) and scanning electron microscopy (SEM; Hitachi S-800). Overall phase composition

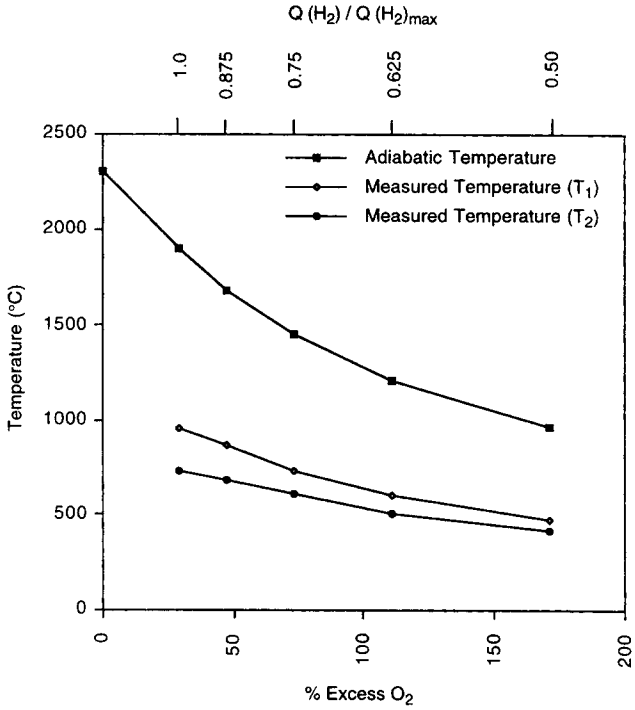

Figure 2. Approximate flame temperature with increasing excess oxygen and decreasing normalized hydrogen flow.

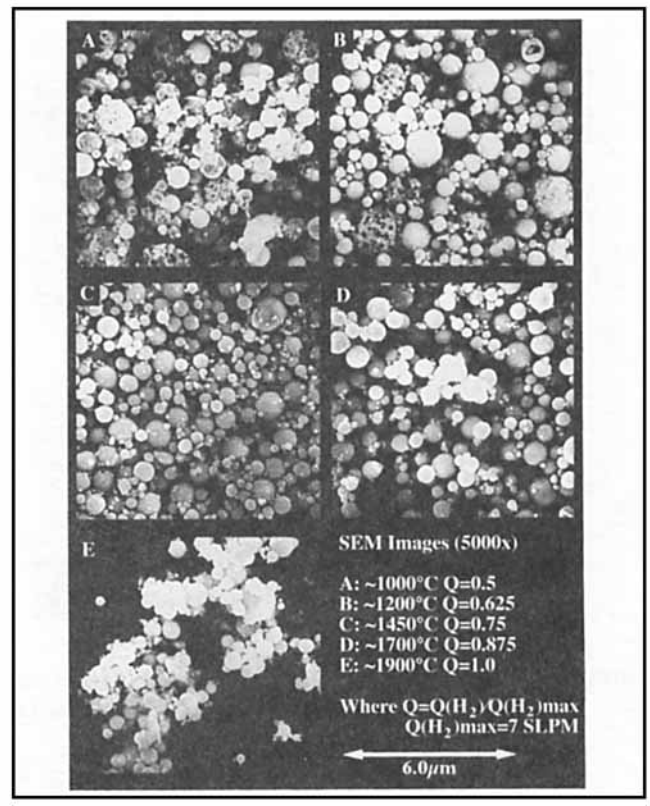

Figure 3. Scanning electron micrographs of barium titanate powders showing a transition from porous to solid particles with increasing adiabatic flame temperature.

and crystallinity were determined by X-ray diffraction (XRD; Scintag/USA diffractometer; CuK_α X-rays). Elemental analysis was accomplished by Auger electron spectroscopy (AES; PHI 10-155 cylindrical mirror analyzer; acceleration voltage = 3 keV). Particle-size distributions were measured using sedimentation velocity analysis (SediGraph 5100; Micromeritics). Multipoint Brunauer, Emmett, and Teller (BET) analysis (GEMINI 2360; Micromeritics) was implemented in order to determine the surface area of the $BaTiO_3$ particles.

Results and Discussion

Scanning electron micrographs of barium titanate particles formed at a relatively low flame temperature ($< \sim 1{,}000$°C) showed that the particles produced were not fully melted and were asymmetrical (Figure 3a). Some particles formed under these conditions exhibited a hollow, porous morphology. As the flame temperature was increased, a transition region was discovered for the temperature where more particles with smooth, spherical morphology were observed. At the higher flame temperatures ($> \sim 1{,}500$°C), the particles produced were dense, spherical, and had smooth surfaces. Overall, the particle-size distributions were determined by the droplet distributions produced by the ultrasonic nebulizer.

At a fixed temperature, variation of the residence time through the flame exhibited similar effects as flame temperature. That is, as residence time increased, particles underwent a transition from rough, asymmetrical, and porous, to smooth, spherical, and dense. Figure 3 shows SEM micrographs of the effect of flame temperature on particle morphology. Figure 4 is a transmission electron micrograph (TEM) image of dense $BaTiO_3$ particles formed at ~ 1900°C [adiabatic (ad.)].

Particles shown in Figures 3a and 3b exhibited rough, porous morphology due to rapid formation at temperatures lower than the material's melting point. Some of the particles in Figures 3a and 3b passed through hotter regions within the flame, which enabled them to partially melt and densify. Particles shown in Figures 3c, 3d and 3e were formed at temperatures above the melting point of barium titanate, where aerosol densification readily occurred. As shown in Figure 4, at high temperature, the formation of some nanosized particles also occurred. This may be due to vapor-phase formation of $BaTiO_3$ or due to the extremely high heating rate ($\sim 10^7$°C/s) causing some of the precursor droplets to explode.

The effect of flame temperature on the powder surface area is shown in Figure 5. The particles formed at low temperature ($< \sim 1{,}000$°C ad.) exhibited the highest surface area (3.1 m^2/g, according to BET multipoint analysis) due to their rough morphology. At $\sim 1{,}200$°C, the surface area reduced to 0.87 m^2/g, showing a transition from rough, porous particles to solid, spherical particles. The surface area was minimized to 0.34 m^2/g at an adiabatic flame temperature of around 1,450°C. This is close to the theoretical value for dense spheres of $BaTiO_3$ particles with an average diameter of 1.4 μm. As the flame temperature increased beyond 1,500°C (ad.), the BET surface area gradually increased to 1.1 m^2/g

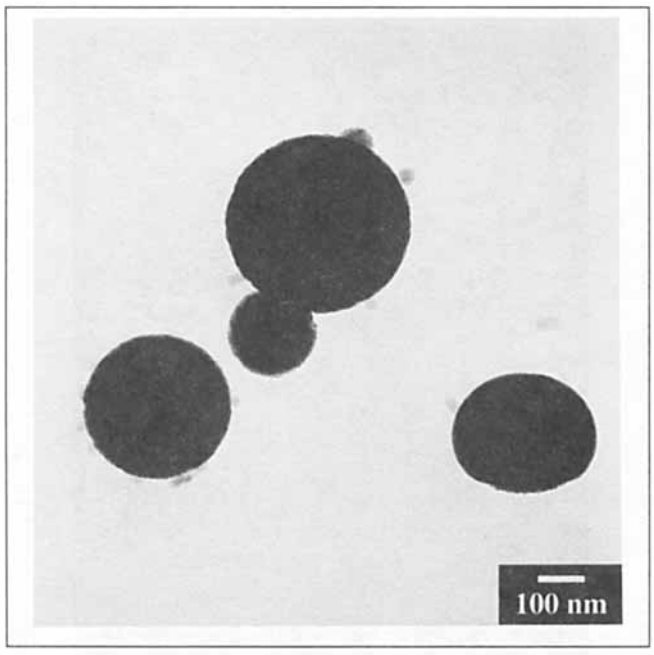

Figure 4. Transmission electron micrograph of barium titanate powder produced at ~1,900°C (adiabatic flame temperature).

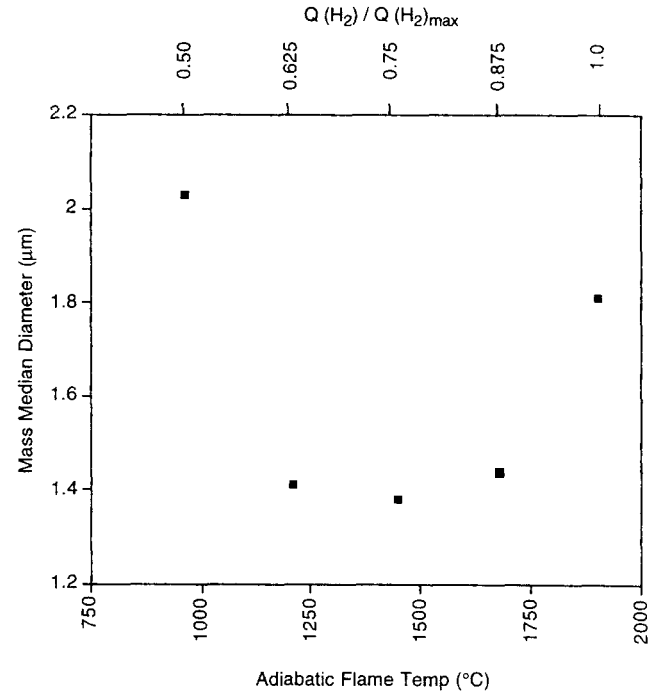

Figure 6. Mass median diameter of barium titanate powder with increasing flame temperature.

at ~ 1,900°C (ad.). This increase may be due to the formation of nanosized particles at high temperatures (> 1,500°C). The presence of these particles was detected by SEM and TEM; however, they were too small to be analyzed by sedimentation velocity analysis. These results were consistent with both vapor-phase formation of nanosized $BaTiO_3$ particles and the formation of submicrometer-sized particles by precursor explosion due to high heating rates.

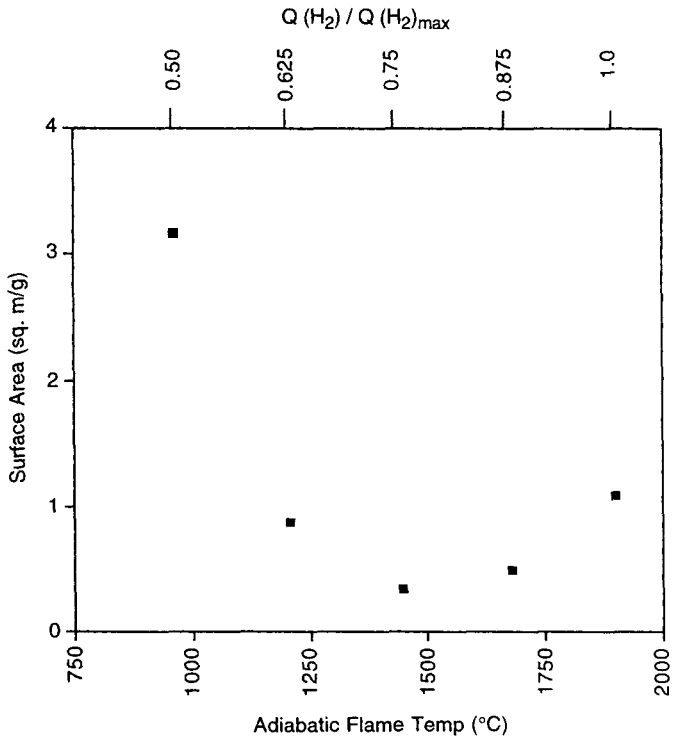

Figure 5. Surface area of barium titanate powders with increasing flame temperature.

Particle-size distributions were obtained by sedimentation velocity analysis. Figure 6 shows the relationship between the mass median diameter (MMD) of the $BaTiO_3$ particles (calculated assuming dense particles) and the adiabatic flame temperature at which they were formed. Showing a similar trend as the surface area vs. flame temperature, the MMD of the particles formed at low temperature (~ 1,000°C ad.) was approximately 2.0 μm. The MMD decreased to around 1.4 μm in size for adiabatic flame temperatures between 1,200 and 1,700°C. This decrease in average size was due to complete particle densification. When barium titanate particles were formed at high temperature (~ 1,900°C ad.), the MMD increased to around 1.8 μm. However, this powder contained the highest quantity by mass (~ 3.5%) of particles below the 100-nm range. The result of the MMD equaling 1.8 μm for particles formed at high temperature was not supported by SEM or TEM analysis. All other results obtained from sedimentation-velocity analysis were confirmed by SEM and TEM. The increase in the measured MMD was most likely an artifact caused by the presence of the nanosized particles.

According to X-ray diffraction (XRD) results, shown in Figure 7, for all investigated temperatures (~ 1,000–2,000°C ad.), the powder was crystalline. Neglecting the strain terms, the crystalline structure was primarily the tetragonal phase along with the hexagonal and cubic polymorphs of $BaTiO_3$. High-temperature (> 1,400°C) hexagonal phase was present due to rapid quenching of the $BaTiO_3$ particles. This phase is not desirable for the final sintered ceramic present in ferroelectric applications. However, under typical sintering conditions, the hexagonal phase is not thermodynamically fa-

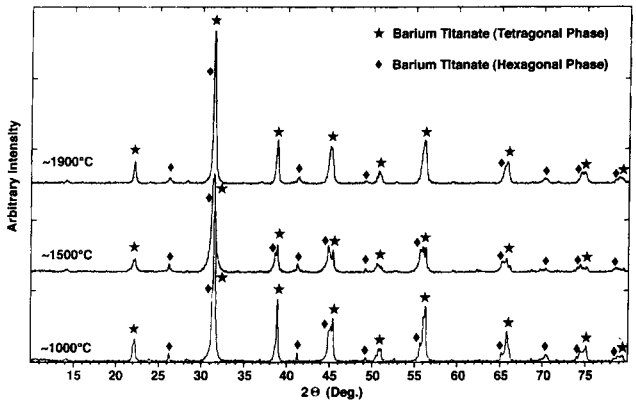

Figure 7. X-ray diffraction patterns of barium titanate powder formed at various adiabatic flame temperatures.

vored and would be converted to the desired tetragonal phase. Neglecting the strain terms, the crystallite size was calculated using the full width at half-max (FWHM) of the deconvoluted 110, 111 and 200 peaks of the tetragonal phase and applying Scherrer's formula:

$$t = \frac{0.9\lambda}{\beta \cos(\theta_{\text{peak}})}. \qquad (2)$$

Using this method, the average crystallite size was approximately 90 nm. Crystallite size was not significantly affected by variations in temperature or residence time. This is because the particles melted and were cooled at similar rates. Conceptually, the crystallite size can be controlled by altering the rate at which the particles are cooled from the liquid phase to the solid phase. In conventional spray pyrolysis, in order to densify hollow and/or porous particles, the temperature and/or residence time must be increased. In doing this, crystallite growth occurs that in some cases may be undesirable.

Particle stoichiometry was analyzed by Auger electron spectroscopy (AES). The results of this surface-sensitive technique indicated that the atomic Ba:Ti:O ratio was 1:1:3 at the surface. After 5 min (corresponding to ~ 10 nm) of material removal by Ar^+ ion beam (ion beam intensity = 10 μA/cm^2 at 1 keV), the ratio remained 1:1:3. Further subtractive sputtering was not attempted due to preferential Ba removal (established by sputtering a stoichiometric standard). From these data and information provided by XRD, it was concluded that an atomic ratio of Ba:Ti:O = 1:1:3 was maintained throughout the powder for all temperatures and residence times examined. This indicated that no separate regions of TiO_2 or BaO were present, the particles were chemically pure, and provides evidence that particles were not formed from the vapor phase because no phase segregation was observed.

Conclusions

Dense, spherical, unagglomerated $BaTiO_3$ particles can be produced using flame-spray pyrolysis. Furthermore, particles with varying morphologies could be produced by varying flame temperature and/or particle residence time through the flame. When compared to particles formed by conventional spray pyrolysis using a tubular furnace, $BaTiO_3$ particles generated using a high-temperature flame reactor were more suitable for use as a sintered ceramic material. As this work demonstrated, flame-spray pyrolysis is the only way to produce dense barium titanate particles via an aerosol route. This is because the high heating rates along with higher temperature associated with flame-spray pyrolysis allow the particles to densify more rapidly than when formed in a tubular reactor. This simple process has the potential for broad use in producing a wide variety of ceramic and metallic powders.

Notation

d = flow diameter of aerosol stream, cm
L = flame length, cm
Q = volumetric flow rate of aerosol stream, cm^3/s
t = average crystallite size, Å
T_1 = reference temperature taken at location T_1 (Figure 1)
T_2 = reference temperature taken at location T_2 (Figure 1)
T_i = inlet temperature of aerosol stream, °C
T_f = estimated flame temperature, °C
β = 0.5(FWHM) (rad)
λ = 1.5405 Å (wavelength of CuK_α X-ray)
θ_{peak} = the angle at which the peak occurred

Literature Cited

Arlt, G., D. Hennings, and G. de With, "Dielectric Properties of Fine-Grained Barium Titanate Ceramics," *J. Appl. Phys.*, **58,** 1619 (1985).

Buchanan, R. C., and J. Boy, "Effect of Powder Characteristics on Microstructure and Properties in Alkoxide-Prepared PZT Ceramics," *J. Electrochem. Soc.*, **132,** 1671 (1987).

Colomban, P., "Chemical and Sol-Gel Processes—The Elaboration of Ultrafine Powders," *Ind. Ceram.*, **792,** 186 (1985).

Edelson, L. H., and A. M. Glaeser, "Role of Particle Substructure in the Sintering of Monosized Titania," *J. Amer. Ceram. Soc.*, **71,** 225 (1988).

Fang, T. T., H. B. Lin, and J. B. Hwang, "Thermal Analysis of Barium Titanate Prepared by Coprecipitation," *J. Amer. Ceram. Soc.*, **73,** 3363 (1990).

Gurav, A., T. T. Kodas, T. Pluym, and Y. Xiong, "Aerosol Processing of Materials," *Aerosol Sci. Technol.*, **19,** 411 (1993).

Kinoshita, K., and A. Yamaji, "Grain-Size Effects on Dielectric Properties in Barium Titanate Ceramics," *J. Appl. Phys.*, **47,** 371 (1976).

Kodas, T. T., "Generation of Complex Metal Oxides by Aerosol Processes: Superconducting Ceramic Particles and Films," *Adv. Mater.*, **1,** 180 (1989).

Lee, H. G., and H. O. Kim, "Ceramic Particle Size Dependence of Dielectric and Piezoelectric Properties of Piezoelectric Ceramic-Polymer Composites," *J. Appl. Phys.*, **67,** 2024 (1990).

Ortega, J., T. T. Kodas, S. Chadda, D. M. Smith, and M. Ciftcioglu, "Formation of Dense $Ba_{0.86}Ca_{0.14}TiO_3$ Particles by Aerosol Decomposition," *Chem. Mater.*, **3,** 746 (1991).

Rossetti, G. A., Jr., J. L. Burger, and R. D. Sisson, Jr., "Characterization of Mixed Cobalt-Molybdenum Oxides Prepared by Evaporative Decomposition of Solutions," *J. Amer. Ceram. Soc.*, **72,** 1811 (1989).

Zachariah, M., and S. Huzarewicz, "Aerosol Processing of YBaCuO Superconductors in a Flame Reactor," *J. Mater. Res.*, **6,** 264 (1991).

Manuscript received Oct. 28, 1996, and revision received June 4, 1997.